

A suppressor of multiple extracellular matrix-degrading proteases and cancer metastasis

Lan Ian Yin^{a, b, #}, Chin Man Chung^{b, #}, Jie Chen^{b, #}, Kin Lam Fok^b, Chuen Pei Ng^b, Rui Rui Jia^b, Xuan Ren^a, Jiannong Zhou^c, Tong Zhang^c, Xiao Hang Zhao^d, Min Lin^b, Hu Zhu^{a, b}, Xiao Hu Zhang^b, Lai Ling Tsang^b, Ye Bi^a, Zuomin Zhou^a, Fugen Mo^c, Nathalie Wong^e, Yiu Wa Chung^b, Jiahao Sha^{a, *}, Hsiao Chang Chan^{b, *}

^a Laboratory of Reproductive Medicine, Nanjing Medical University, Nanjing, China

^b Epithelial Cell Biology Research Center, Li Ka Shing Institute of Health Sciences, Department of Physiology, Faculty of Medicine, The Chinese University of Hong Kong, Shatin, Hong Kong

^c Department of Pathology, Jiangsu Cancer Hospital, Nanjing, China

^d National Laboratory of Molecular Oncology Cancer Institute and Hospital, Academy of Medical Sciences and Peking Union Medical College, Beijing, China

^e Department of Anatomical and Cellular Pathology, Faculty of Medicine, The Chinese University of Hong Kong

Received: September 16, 2008; Accepted: October 17, 2008

Abstract

Cancer metastasis remains the most poorly understood process in cancer biology. It involves the degradation of extracellular matrix (ECM) proteins by a series of 'tumour-associated' proteases. Here we report the identification of a novel protease suppressor, NYD-SP8, which is located on human chromosome 19q13.2. NYD-SP8 encodes a 27 kD GPI-anchored cell surface protein, which shows structural homology to urokinase plasminogen activator receptor (uPAR). Co-immunoprecipitation experiments showed that NYD-SP8 binds to uPA/uPAR complexes and interfere with active uPA production. Overexpression of NYD-SP8 results in reducing activities of the three major classes of proteases known to be involved in ECM degradation, including uPA, matrix metalloproteinases (MMPs) and cathepsin B, leading to suppression of both *in vitro* and *in vivo* cancer cell invasion and metastasis. These data demonstrate an important role of NYD-SP8 in regulating ECM degradation, providing a novel mechanism that modulates urokinase signalling in the suppression of cancer progression.

Keyword: extracellular matrix • glycosylated phosphatidylinositol • urokinase plasminogen activator receptor • proteases inhibitor

Introduction

Metastasis is the major cause of death for most cancer patients [1], which is accompanied by the degradation of extracellular matrix (ECM) by a series of 'tumour-associated' proteases. These proteases, according to the catalytically active site, are classified into three major classes: serine proteases (such as uPA) [2], cysteine proteases (cathepsins) [3, 4] and metalloproteinases (MMPs) [5, 6]. Targeting these proteases is a promising strategy for anti-cancer therapy. There are some

inhibitors, such as uPA specific inhibitor (PAI), proven effective in experimental models; however, they exhibited a lack of efficacy in the anti-cancer treatment in the clinical setting. Cloning and identification of novel genes that may critically affect proteolytic degradation is needed.

Materials and methods

Animals

Nude mice were purchased from Laboratory Animal Service Center (LASEC), The Chinese University of Hong Kong. All experimental procedures were under ethical approval from LASEC (ethical no. 06/049/MIS).

[#]These authors contributed equally in this project.

*Correspondence to: Hsiao Chang CHAN,
Department of Physiology, Faculty of Medicine,
The Chinese University of Hong Kong, Shatin, Hong Kong SAR
Tel.: +852 2609 6001
Fax: +852 2603 7155
E-mail: hsiaocchan@cuhk.edu.hk

doi:10.1111/j.1582-4934.2008.00576.x

Cell lines and transfection

Human hepatocellular carcinoma cell line (hHCC) and human nasopharyngeal cancer cell lines (CNE1) were cultured in RPMI 1640 (Gibco, Carlsbad, CA, USA) supplemented with 10% heat-inactivated FBS and antibiotics. For overexpression, NYD-SP8 was PCR amplified using forward primer 5'-5'-ATTGTCCAGCACTCTTACC-3' and reverse primer 5'-AGAGACTCAATGCCACC-3' and PCR products were subsequently cloned into GFP-fusion overexpression vector (Clontech, Palo Alto, CA, USA). Transfection was performed using Lipofectamine reagent (Invitrogen, Carlsbad, CA, USA). In total, 500 µg/ml G418 were used to establish stable transfected cell lines.

Preparation of recombinant NYD-SP8 protein, antibodies and immunohistochemical detection

The cDNA fragment corresponding to amino acids 25–184 of the protein amplified by PCR and subsequently subcloned into the pET28a vector (Novagen, Madison, WI, USA) and expressed in E.Coli BL21 CodonPlus[®]DE3 RP (Stratagene, La Jolla, CA, USA). The recombinant protein was affinity purified with a Ni-nitrilotriacetic acid (NTA) column and renatured by dialysis. And then, purified NYD-SP8 protein was used for mouse immunization and subsequent boosts (100 mg each) in incomplete adjuvant. After serum titres and specificity were tested by ELISA and Western blot respectively, NYD-SP8 antibody was purified using Montage Antibody Purification Kits (Millipore, Billerica, MA, USA) for immunohistological detection according to the manufacturer's instructions of PicTure(tm)-Plus Kit (ZYMED/Invitrogen) and in subsequent experiment. Antibodies for uPAR3937 and uPAR399R were purchased from American Diagnostics Inc. (American Diagnostic Inc, Greenwich, CT, USA). Antibodies for uPA (H-140); antibodies for uPAR(FL-290), uPA(H-140) and β-tubulin were purchased from Santa Cruz (Santa Cruz, Santa Cruz, CA, USA).

RT-PCR

Total RNA for analysis was isolated using Trizol (Invitrogen). For reverse transcription and amplification, we use oligo(dT) primer and M-MLV reverse transcriptase (Life Technologies, Cergy Pontoise, France). Amplified product was separated through 2% agarose gel and visualized on an ultraviolet transilluminator.

Western blot

Cells were lysed and 40 µg of proteins were separated by 8% or 12% SDS-PAGE. Western blots were probed with the indicated antibodies. For all Western blots, representative examples of at least three independent experiments are shown.

Co-immunoprecipitation

For co-immunoprecipitation experiments, we harvested cell lysate in ice-cold 0.2% Triton X-100 buffer for 30 min. Antibody against NYD-SP8 and uPAR399R (5 µg per reaction) were incubated together with cell lysate

and protein G-Sepharose (Amersham Biosciences, Amersham, UK) overnight at 4°C. After immunoprecipitation, we thoroughly washed the beads, and analysed bound proteins by immunoblot using monoclonal antibody to NYD-SP8, uPAR and uPA at a dilution of 1:500, 1:1000 and 1:1000, respectively.

uPA activity assay

uPA activity was examined using uPA activity assay kit (Chemicon, Temecula, CA, USA) according to the manufacturer's instruction. Results were obtained after 24 hrs of incubation. The photometric absorbance of the reaction mixtures at 405 nm was measured using a SpectraMax ELISA reader (MVG Biotech, Ebersberg, Germany). Data were shown as three separate experiments and each of which is in triplicate.

Gelatin zymography

Enzymatic activities of MMP2 and MMP9 were detected by gelatin zymography. Same numbers of NYD-SP8-stably expressing hHCC lines and its control were incubated in equal amount of serum-free media for 24 hrs and same volume of conditioned media was separated by 7.5% SDS-PAGE gels containing 0.1% gelatin (Sigma, St.Louis, MO, USA) under non-reducing conditions. Gels were washed twice with 2.5% (v/v) Triton X-100, then incubated in zymography digestion buffer (200 mM NaCl, 50 mM Tris, 5 mM CaCl₂, 0.2M NaCl₂, 0.02% (v/v) Brij-35) for 18 hrs at 37°C. Gels were stained in 0.5% Coomassie Blue R-250 solution for 2 hrs, then destained. Area of clear bands against a blue background indicates the activities of proteases. Experiment was done in triplicate.

Cathepsin B activity assay

Cathepsin B activity in protein lysates was measured using the InnoZyme[™] Cathepsin B activity Assay Kit, Fluorogenic (Calbiochem, San Diego, CA, USA) according to manufacturer's instructions. In brief, cell pellets were lysed in MES buffer (pH 6.0, containing EDTA) and the enzyme activity was determined by using the specific substrate Z-Arg-Arg-AMC. Results were displayed as fluorescence units/µg total protein/time. Data were shown as three separate experiments and each of which is in triplicate.

Matrigel invasion assay

The *in vitro* invasion potential of cancer cells were determined using Cell Invasion assay kit, Fluorogenic (Chemicon) according to manufacturer's instructions. Results were obtained 48 hrs after incubation. Data were shown as three separate experiments, each of which is in triplicate.

Fluorescent labelling

Cells were incubated together with fluorescent cell tracker dyes CMRA (a rhodol-based fluorophore, red fluorescent) or CMFDA (5-chloromethyl-fluorescein diacetate, green fluorescent) at 2 µM (Molecular Probes, Eugene, OR, USA) according to manufacturer's instruction. After washing, cells were incubated for an additional 30 min. with dye-free medium, washed and trypsinized.

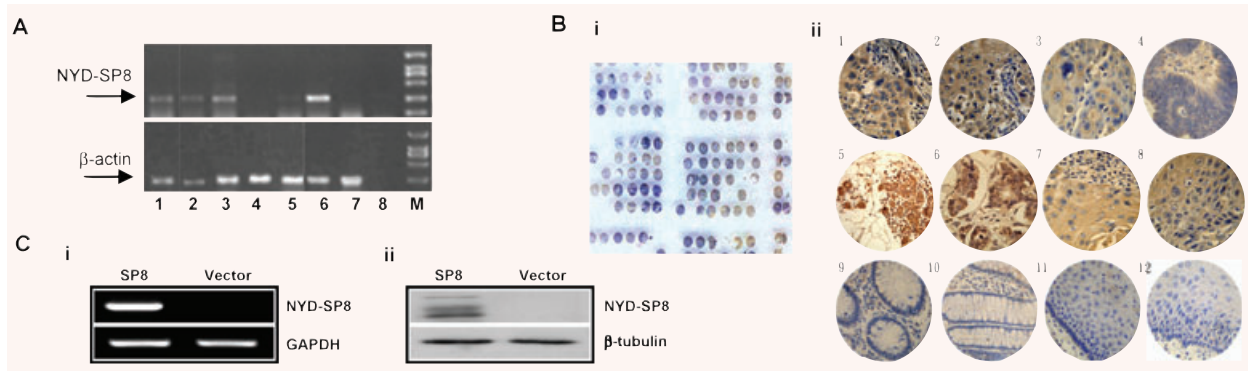


Fig. 1 Characterization of NYD-SP8 (A) RT-PCR analysis of NYD-SP8 mRNA expression levels in malignant lymphoma (1); adenocarcinoma of kidney (2); colon cancer (3); mastocytosis (4); lung cancer (5); oesophageal cancer (6); gastric carcinoma (7); negative control (8). β -actin was used as internal control. (B) (i) Immunohistochemical demonstration of NYD-SP8 protein expression in multiple human cancer tissue arrays. (ii) Representative fields from (i) with various cancer tissues and their normal tissues counterparts: cervical cancer (1–2), pudendum cancer (3), colon cancer (4), lung cancer (5), breast cancer (6), oesophageal squamous cell carcinoma ESCC (7–8), normal colon mucosa (9–10); normal oesophageal mucosa (11–12). All photos were taken at $400\times$. (C) (i) RT-PCR and (ii) Immunoblot of hHCC clones stably expressing NYD-SP8 (SP8) or empty vector (Vector).

In vivo metastasis assay

For tumour carcinomatosis assay, 5×10^5 tumour cells were injected intra-peritoneal into the abdomen cavity of nude mice. After 60 days, mice were sacrificed and the lungs from each group of mice were excised and RT-PCR was performed.

For experimental metastasis assay, hHCC/SP8 or hHCC/vector were labelled *in vitro* with CMRA or CMFDA as described above. Cell labelled with red and green fluorescent dyes were mixed at a ratio of 1:1. Approximately 2×10^6 cells suspended in HBSS were injected iv by tail vein. The ratio of green-to-red fluorescence tumour cells in the injected suspensions was measured by counting in a fluorescence microscope. Lung were harvested at 10 min. or 6 hrs after injection. The trachea and pulmonary artery were cannulated and perfused *in situ* with ice-cool $1 \times$ PBS followed by 4% Paraformaldehyde (in PBS) gently. Lung tissues were sectioned at $5 \mu\text{m}$ in a cryostat and fluorescent cells in 15 random fields of each slice were counted.

Statistical analysis

All data are expressed as mean \pm S.E.M. or \pm S.D. ($n = 3$ or more). Statistical analysis was performed using Student's t-test and analysis. Results are representative examples of more than three independent experiments, each with triplicates. $P < 0.05$ are considered to be significant.

Results and discussion

Identification and characterization of NYD-SP8

In this study, a novel gene, NYD-SP8 (Gene bank Accession No. AY014285.1), was identified and characterized from cDNA

microarray hybridization [7]. NYD-SP8 exhibited a 7-fold higher expression in adult testis than that in embryo testis (Fig. S1A). The use of the RH position markers placed the gene in human chromosome *19q13.2* where many CT genes have been mapped. This prompted us to investigate the mRNA expression of NYD-SP8 in both normal and cancer tissues. RT-PCR analysis revealed that NYD-SP8 mRNA was predominantly expressed in the testis but not other organs examined (Fig. S1B). However, NYD-SP8 mRNA was expressed in a number of cancer tissues from human patients including lymphoma, and adenocarcinoma of kidney, carcinomas of the colon and oesophagus (Fig. 1A). Results of immunohistochemical studies of multiple human cancer tissue arrays (Fig. 1B-i) also showed that NYD-SP8 protein was expressed in different cancer tissues, including lung cancer, breast cancer, pudendum cancer, colon cancer and oesophagus squamous cell carcinoma, but not detected in their normal tissue counterparts (Fig. 1B-ii). These results are consistent with a recent report showing that a homologue of NYD-SP8 in mice was expressed in some small cell lung cancer [8], indicating a possible role of NYD-SP8 in cancer development.

Bioinformatic studies showed that NYD-SP8 is a putative GPI-anchored membrane protein (<http://www.ebi.uniprot.org>), with about 30% homology to urokinase Plasminogen Activator Receptor (uPAR) (Fig. S2), which is important in converting plasminogen to active plasmin and promoting the degradation of ECM [9]. Once bound to uPAR, uPA is activated and turning on subsequent proteolytic cascades [10], which have been implicated in cancer invasion and metastasis of a variety of cancers [11]. We thus raised the question: could it be possible that NYD-SP8 is involved in the uPA/uPAR-mediated ECM degradation during cancer metastasis?

To answer this question, we employed a human hepatocellular carcinoma cell line (hHCC), which is highly invasive and does not have detectable endogenous NYD-SP8. We stably transfected

NYD-SP8 (hHCC/SP8) or its vector control (hHCC/vector) into these cells. Expression of NYD-SP8 was confirmed by RT-PCR and Western blot (Fig. 1C).

NYD-SP8 interacts with uPA/uPAR complexes and suppresses uPA activity

We then examined possible protein–protein interaction of NYD-SP8 with uPA/uPAR system by performing co-immunoprecipitation experiments. The results showed that NYD-SP8 could pull down both uPA and uPAR in hHCC/SP8 (Fig. 2A-i), suggesting that NYD-SP8 interacts with the uPA/uPAR complexes, which may interfere with the downstream signalling of uPAR-mediated uPA activation. Similarly, anti-uPAR antibody, but not anti-IgG, could pull down both NYD-SP8 and uPA in hHCC/SP8 (Fig. 2A-ii), further confirming protein–protein interaction between uPA/uPAR complexes and NYD-SP8.

We further examine possible effect of NYD-SP8 on uPA/uPAR system using uPA activity assay kit (Chemicon) and Western blot. The results showed significant reduction in the uPAR-mediated active uPA production in hHCC/SP8 cells as compared to vector control cells, (** $P < 0.01$, Fig. 2B-i). This could be reversed by anti-NYD-SP8 antibody, but not control IgG antibody, at a concentration of 5 $\mu\text{g/ml}$ (** $P < 0.01$, Fig. 2B-i), suggesting that the suppressing effect of NYD-SP8 on active uPA production *in vitro* was specific. This was further confirmed by the use of recombinant NYD-SP8, showing concentration-dependent reduction in active uPA production with increasing amount of NYD-SP8 used (Fig. 2B-ii). Interestingly, NYD-SP8 antibody, but not IgG, also produced an increase in uPA activity in a nasopharyngeal cancer cell line (CNE1) expressing endogenous NYD-SP8 (Fig. S3), consistent with an inhibitory role of NYD-SP8 in the uPA/uPAR system. Similar results were observed using Western blot, with less active uPA detected in the NYD-SP8-expressing cells (Fig. 2C-i) and when excess recombinant NYD-SP8 was added (20 $\mu\text{g/ml}$), active uPA production could also be blocked (Fig. 2C-ii), consistent with that revealed by uPA activity assay (Fig. 2B-ii). However, no significant alternations in pro-uPA and uPAR expression were observed (Fig 2C-i). Interestingly, when recombinant NYD-SP8 protein was added into culture medium, a diffuse band of ~120–160 kD was observed in all the NYD-SP8-treated, but not BSA-treated, samples under non-denaturing and non-reducing conditions, indicating complex formation between NYD-SP8 with uPA/uPAR complexes (Fig. 2C-ii). Taken together, these results indicate that NYD-SP8 could bind to uPA/uPAR complexes, thereby interfering with uPA/uPAR activation process and leading to the observed decrease in active uPA production in NYD-SP8-overexpressed or NYD-SP8-treated cells.

We also tested whether NYD-SP8 could affect uPA-related genes expression at transcript level. Semi-quantitative RT-PCR results showed that there was no significant difference in the mRNA expression profiles of uPA, uPAR and uPA specific inhibitor (PAI-1) between hHCC/SP8 and hHCC/vector cells (Fig. 2D), suggesting that the decrease in active uPA production in the NYD-

SP8 expressing cells was not due to transcriptional change in the uPA/uPAR system.

NYD-SP8 suppresses MMPs and cathepsin B activities

It is established that the binding of uPA to uPAR activates the conversion of plasminogen to plasmin, and thereby enhancing ECM degradation through multiple signalling pathways such as promoting the expression/activation of MMPs, which are family of zinc-dependent endopeptidases that have been implicated in the proteolytic events of tumour cell invasion [12]. Among this family, Gelatinases A and B (MMP2 and MMP9) have been shown to play an important role in ECM degradation and participate in cancer progression in several neoplasia [13]. Gelatin Zymography was used to investigate whether NYD-SP8 affects MMPs activities in conditioned medium, and the results showed that both MMP2 and MMP9 activities were reduced in hHCC/SP8 cells with more prominent effect on MMP9 activity (Fig. 3A-i). This was further confirmed by the use of recombinant NYD-SP8, showing significant reduction in both pro- and active MMP9 productions with 10 $\mu\text{g/ml}$ of NYD-SP8 used (Fig 3A-ii). To further assess the nature of NYD-SP8-induced suppression in MMP activities, mRNA expression of MMP2 and MMP9 was measured using semi-quantitative RT-PCR and the results showed that both MMP2 and MMP9 mRNA levels were significantly decreased in hHCC/SP8 (Fig. 3A-iii), indicating a suppressor role of NYD-SP8 in MMPs expression/production.

During cancer metastasis, other proteases, such as cathepsin B, have been demonstrated to mediate direct ECM degradation [14]. Cathepsin B is also suggested to be an important upstream regulator in the activation of pro-uPA, plasminogen and pro-MMPs, thereby indirectly involved in mediating ECM degradation [15]. Because NYD-SP8 appears to interfere with the uPA/uPAR system, it may also affect uPA/uPAR-related cathepsin B activity and ECM degradation. To test this, we measured the cathepsin B activity in hHCC/SP8 and hHCC/vector cells using cathepsin B activity assay kit (Chemicon, San Diego, CA, USA). The results showed that the activity of cathepsin B in hHCC/SP8 was about 10-fold lower than that observed in the vector control (** $P < 0.001$, Fig 3B-i). However, there was no significant alternation in mRNA levels of cathepsin B (Fig. 3B-ii), indicating that NYD-SP8 modified cathepsin B activation at protein level. Taken together, we have demonstrated that NYD-SP8 is a potent suppressor of multiple ECM-degrading proteases, namely uPA, MMPs and cathepsin B, indicating its potential role in suppressing cancer invasion/metastasis.

NYD-SP8 inhibits cancer cell invasion and metastasis *in vitro* and *in vivo*

To examine possible role of NYD-SP8 in suppressing cancer invasion/metastasis *in vitro*, matrigel invasion assay was performed.

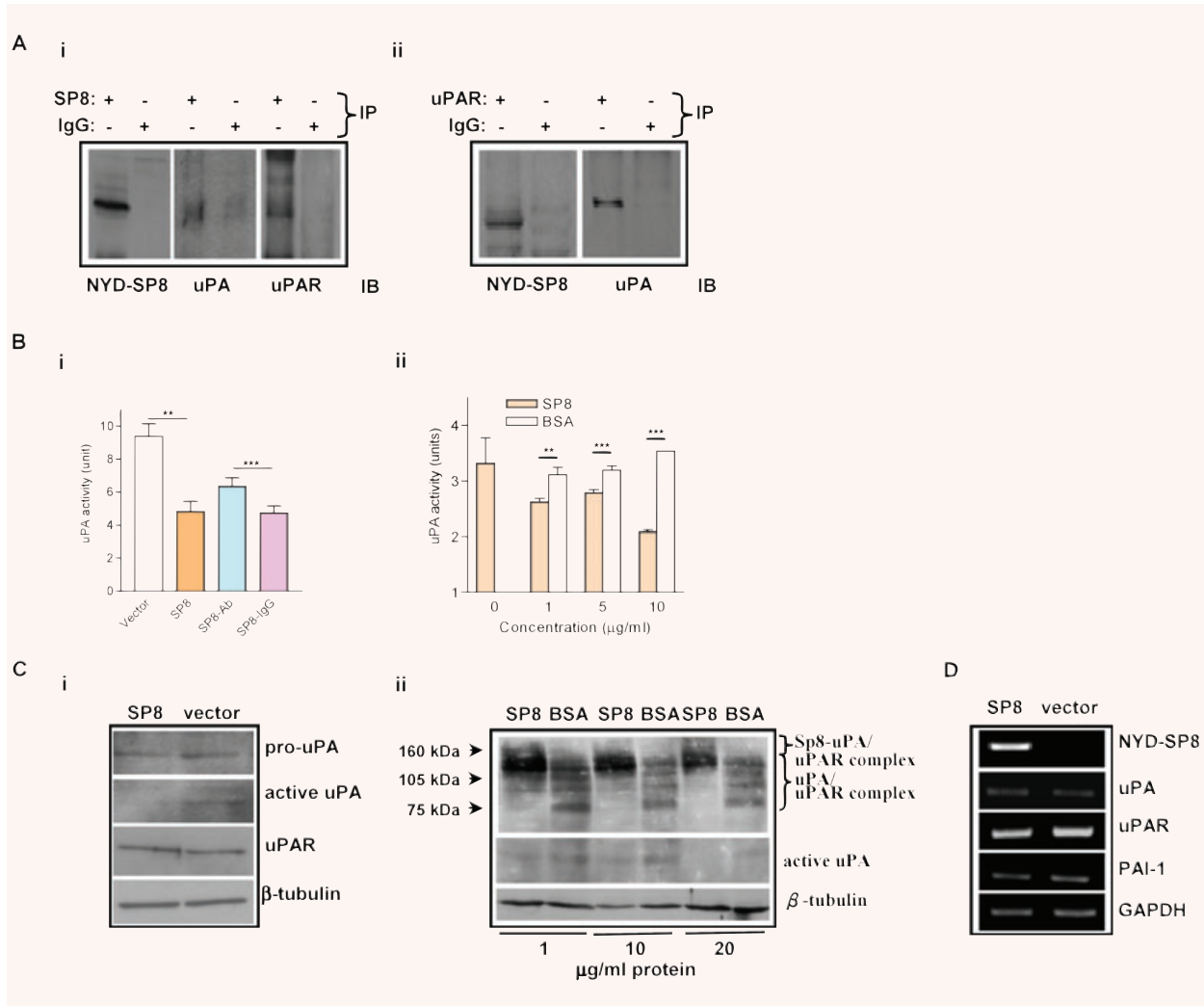


Fig. 2 NYD-SP8 interacts with uPA/uPAR complexes (**A**) Protein–protein interaction between NYD-SP8 and uPA/uPAR complexes. (i) 300 μg of hHCC/SP8 cell lysate were immunoprecipitated (IP) with NYD-SP8 antibody (SP8), resolved by SDS-PAGE and immunoblotted (IB) with NYD-SP8, uPA or uPAR antibodies. (ii) Reversed co-immunoprecipitation of NYD-SP8 and uPA with uPAR. Antibodies for normal mouse or rabbit IgG were used as control correspondingly. (**B**) NYD-SP8 suppresses serine proteases uPA activity at protein level. (i) Comparison of the mean uPA activity in culture medium of hHCC/SP8 cell line (SP8) and its control (Vector), and reversal of uPA activity in the presence of 5 μg/ml of NYD-SP8 antibody (SP8-Ab) but not the normal mouse IgG (SP8-IgG) (values are mean ± S.D., $n = 3$, $***P < 0.001$). (ii) hHCC cells were treated with NYD-SP8 recombinant protein for 24 hrs at indicated concentrations, with corresponding concentrations of BSA as controls, and enzymatic activity of uPA in culture medium was measured. (\pm S.D., $n = 3$, $***P < 0.001$). (**C**) (i) Immunoblot analyses of expression pro-uPA, active uPA and uPAR in hHCC/SP8 cell line (SP8) or its control (Vector) (β -tubulin as a loading control). (ii) hHCC cells were treated with NYD-SP8 recombinant protein for 24 hrs at indicated concentrations, with corresponding concentrations of BSA as controls, and cell lysate were subjected to immunoblot analyses with antibodies to uPA/uPAR complexes, active-uPA or to β -tubulin as a loading control ($n = 3$). (**D**) RT-PCR analysis of mRNA expression of uPA, uPAR and PAI-1 in hHCC/SP8 cell line (SP8) or its control (Vector), with GAPDH as an internal control ($n = 3$).

The results revealed that the invasion capacity of hHCC/SP8 cells was significantly lower by 60% as compared to the vector control ($n = 3$, $**P < 0.01$, Fig. 4A). The NYD-SP8-reduced invasion capacity *in vitro* could be a result from inhibition of ECM degrada-

tion, because NYD-SP8 has potent effects on the three major classes of ECM-degrading proteases.

To further demonstrate the inhibitory effect of NYD-SP8 on cancer invasion/metastasis *in vivo*, we injected hHCC/SP8 into

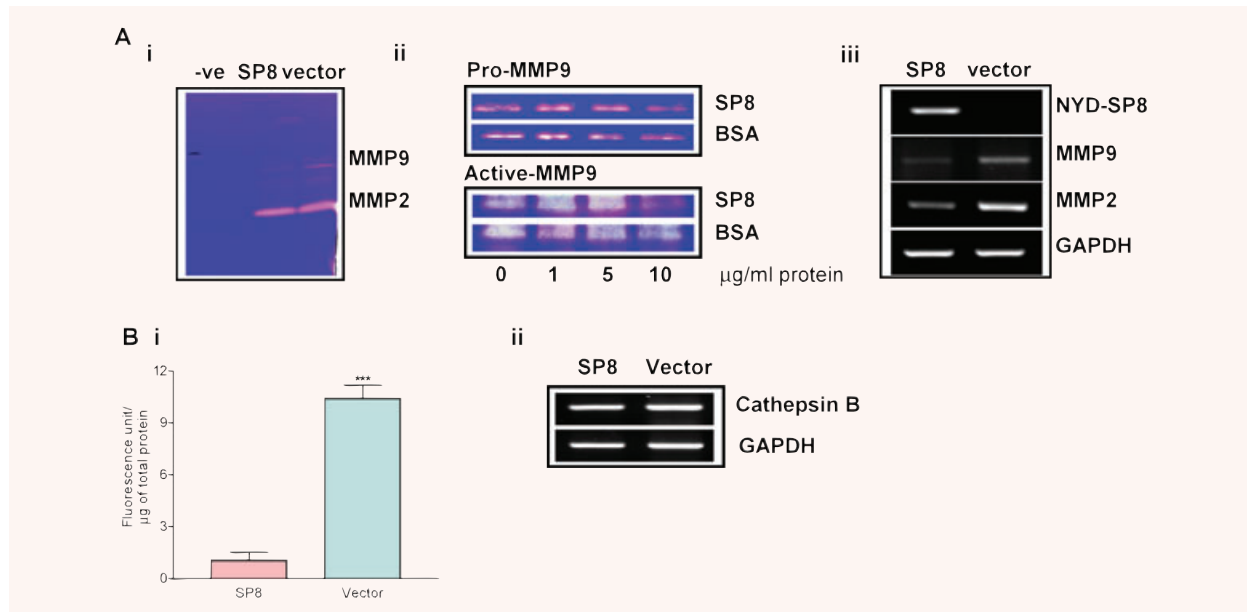


Fig. 3 *In vitro* inhibition of MMPs and cathepsin B activity. (A) NYD-SP8 suppresses MMPs at both transcriptional and protein level. (i) Representative zymographic analysis of active MMP2 and MMP9 release into conditioned media of hHCC/SP8 cell line (SP8) and its control (Vector) ($n = 3$). Negative control lane (-ve) was loaded with conditioned media only. (ii) hHCC cells were treated with NYD-SP8 recombinant protein (SP8) for 24 hrs at indicated concentrations, with corresponding concentrations of BSA as controls, and representative zymographic analyses of MMP9 production conditioned medium are shown ($n = 6$), indicating reduced pro- and active MMP9 with increasing NYD-SP8. (iii) RT-PCR analysis of mRNA expression MMP2 and MMP9 in hHCC/SP8 cells (SP8) or its control (Vector), with GAPDH as an internal control, showing reduced MMPs in hHCC/SP8 cells. (B) Suppressed mean cathepsin B activity (\pm S.D., $n = 3$, $***P < 0.001$) in hHCC/SP8 cell line (SP8) as compared to its control (Vector), with no difference in mRNA expression of cathepsin B (ii) with GAPDH as an internal control.

athymic nude mice by i.p inoculation to examine the presence of metastasized cancer cells in various parts of the body. 5×10^5 cells of hHCC, hHCC/vector and hHCC/SP8 were separately injected into three groups of nude mice intra-peritoneal (i.p) ($n = 12$ /group). All mice receiving hHCC or hHCC/vector inoculation formed tumours (12 out of 12) 30 days after, whereas only 67% (8 out of 12) of mice inoculated with hHCC/SP8 grew tumours (Fig. S4). To examine the effect of NYD-SP8 on tumour invasion, the lungs, hearts and lymph nodes were excised from the nude mice receiving hHCC/SP8 and hHCC/vector i.p. and semi-quantitative RT-PCR was performed to examine the relative expression of human GAPDH, as a metastatic marker, in the organ tissues of the nude mice (Fig. 4B-i). The results showed that hHCC/SP8 treated mice had 50% fewer lung micro-metastasis than that of the vector control (Fig 4B-ii). No significant difference in expression of human GAPDH was detected in the heart between hHCC/SP8 and hHCC/vector (Fig 4B-ii), which could also serve as a control excluding possible contamination of blood vessel perfusion in the observed lung result, suggesting that the presence of human GAPDH in the lung was due to migration and lung extravasations of the human cancer cells. These results have indicated an inhibitory effect of NYD-SP8 on cancer invasion /metastasis *in vivo*.

To further demonstrate the inhibitory effect of NYD-SP8 on cancer metastasis, 2×10^6 of hHCC/SP8 or hHCC/vector cells were injected intravenously (i.v.) into the lateral tail vein of nude mice to produce experimental lung metastasis, bypassing tumour formation at the primary sites. Before i.v. injection, cancer cells (hHCC/SP8 or hHCC/vector) were either stained with the red fluorescent dye CMRA or green fluorescent dye CMFDA and mixed at 1:1 ratio (Fig. 4C-i). Figure 4C-ii and Fig. 4C-iii showed two groups of high magnification fluorescence micrographs of labelled cancer cells in the lungs detected 6 hrs after injection, with consistently fewer hHCC/SP8 detected as compared to the hHCC/vector, regardless of the fluorescent dye used. The total number of cells at 10 min. and 6 hrs after injection was also counted, showing similar cell count in both cases, red or green, at 6 hrs but no fluorescent cells detected in the lungs at 10 min., consistent with insufficient metastasis within this short period of time, which could also serve as a negative control. The demonstrated decrease in cancer invasion/metastasis *in vitro* and *in vivo* in NYD-SP8 expressing cells is consistent with the finding that NYD-SP8 is a potent suppressor of multiple ECM-degrading proteases known to be involved in cancer metastasis.

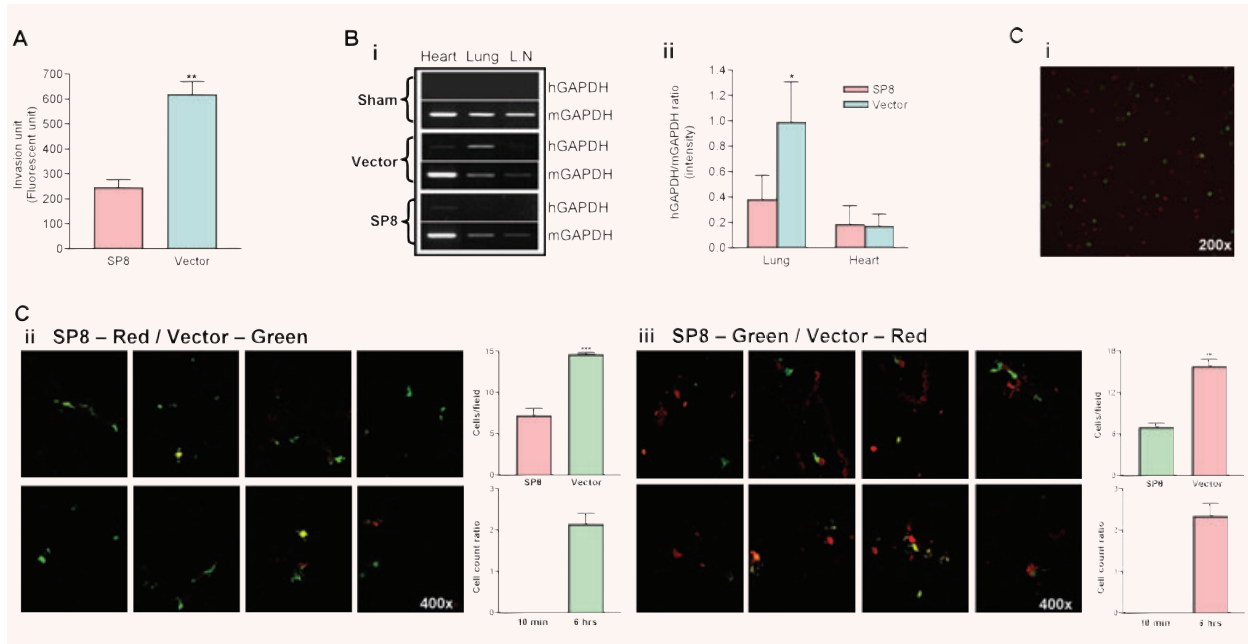


Fig. 4 Suppression of cancer invasion and metastasis *in vitro* and *in vivo*. **(A)** Summary of matrigel invasion assay showing reduced invasion of hHCC/SP8 cell line (SP8) as compared to control (Vector) after 48 hrs of incubation (\pm S.E.M., $n = 3$, $**P < 0.01$). **(B)** NYD-SP8 suppresses experimental metastasis *in vivo*. **(i)** RT-PCR analysis of mRNA expression of human GAPDH (representing the amount of micro-metastasized human cancer cells) in the heart, lung and lymph node (L.N) of mice 60 days after i.p inoculation of hHCC/SP8 cell line (SP8) or its control (Vector), with mouse GAPDH as an internal control. **(ii)** Corresponding quantitative levels of the mean ratio of human GAPDH/mouse GAPDH mRNA in the lungs and hearts as shown in **(i)**, showing significantly higher levels in the lungs of the control group than that of NYD-SP8 group indicating suppressed metastasis by NYD-SP8 (\pm S.D., $n = 3$, $*P < 0.05$). **(C)** Suppressed lung extravasations and metastasis of NYD-SP8-overexpressed cancer cells after tail vein injection. **(i)** Fluorescence microscopy of CMRA-labelled hHCC/SP8 cell line (SP8-Red) mixed in 1:1 ratio with CMFDA-labelled control hHCC cells (Vector-Green) before tail vein injection. The ratio of cell count ratio were measured by counting in a fluorescence microscope. **(ii)** Confocal fluorescence microscopy of randomly selected fields from frozen sections of mouse lungs at 6 hrs after tail vein injection of 1:1 mixed cells with NYD-SP8 (red) and control (green) cells with tumour cell count ratio (green/red) and number of cells per 4 random microscope fields in lung at 10 min. and 6 hrs after tail vein injection. **(iii)** Reversed labelling in **(ii)**. (\pm S.E.M., $n = 3$ for 10 min. group, $n = 6$ for 6 hrs group, $***P < 0.001$).

Conclusion

The demonstrated metastasis-suppressing role of NYD-SP8 and its expression in cancers but not normal tissues except the testis suggest that it could be a host defence mechanism against cancer metastasis. Interestingly, we found that the mRNA expression level of NYD-SP8 in a couple of less invasive hepatocellular cancer cell lines was much higher than its negligible expression in the more invasive hHCC cell line (Fig. S5). This raises an interesting notion that the expression profile of NYD-SP8 may vary with different stages of cancer development and be correlated with different metastatic potentials. Further detailed studies on NYD-SP8 expression profiles in different cancer tissues and the elucidation of the molecular mechanism regulating its expression may provide new insight into cancer development as well as new diagnostic and treatment strategies for cancer metastasis. Although the

detailed mechanisms by which NYD-SP8 suppresses the activities of the three major classes of ECM-degrading proteases require further studies, the presently demonstrated potent inhibitory effects of NYD-SP8 on these proteases as well as cancer invasion/metastasis *in vitro* and *in vivo* indicate its therapeutic potentials for suppressing cancer metastasis.

Acknowledgements

The work was supported by a grant from China National 973 project 2006CB504002, The National Natural Science Foundation of China (30425006, 30630030 and 3057543), Li Ka Shing Institute of Health Science and Focused Investment of The Chinese University of Hong Kong and MorningSide Foundation. H.C. Chan received support from the Croucher Senior Research Fellowship.

Supporting Information

Additional Supporting Information may be found in the online version of this article:

Fig. S1 cDNA microarray hybridization showing 7 fold-higher expression of NYD-SP8 in adult (ii) than the embryo testis (i) (**A**). Testis-specific tissue distribution of NYD-SP8 tested by RT-PCR, with G3PDH as control (**B**).

Fig. S2 Clustal W alignment showing about 30% homology of NYD-SP8 to uPAR.

Fig. S3 NYD-SP8 antibody reversed the uPA activity in nasopharyngeal cancer cell line (CNE1) expressing endogeneous NYD-SP8.

Fig. S4 Bar chart showing the percentage of nude mice forming tumors 30 days after ip inoculation. All mice receiving hHCC or

hHCC/vector inoculation formed tumors (12 out of 12) while only 67% (8 out of 12) of mice inoculated with hHCC/SP8 grew tumors.

Fig. S5 mRNA expression of NYD-SP8 in hHCC, 8024 and 7721 hepatocellular cancer cell lines and a patient sample of late stage of hepatocarcinoma, with GAPDH as control.

This material is available as part of the online article from: <http://www.blackwell-synergy.com/doi/abs/10.1111/j.1582-4934.2008.00576.x>

(This link will take you to the article abstract).

Please note: Blackwell publishing are not responsible for the content or functionality of any supporting materials supplied by the authors. Any queries (other than missing material) should be directed to the corresponding author for the article.

References

1. **Singh S, Singh UP, Stiles JK, et al.** Expression and functional role of CCR9 in prostate cancer cell migration and invasion. *Clin Cancer Res.* 2004; 10: 8743–50.
2. **Schmitt M, Janicke F, Moniwa N, et al.** Tumor-associated urokinase-type plasminogen activator: biological and clinical significance. *Biol Chem Hoppe Seyler.* 1992; 373: 611–22.
3. **Mackay AR, Corbitt RH, Hartzler JL, et al.** Basement membrane type IV collagen degradation: evidence for the involvement of a proteolytic cascade independent of metalloproteinases. *Cancer Res.* 1990; 50: 5997–6001.
4. **Blasi F, Carmeliet P.** uPAR: a versatile signalling orchestrator. *Nat Rev Mol Cell Biol.* 2002; 3: 932–43.
5. **Schmitt M, Janicke F, Moniwa N, et al.** Tumor-associated urokinase-type plasminogen activator: biological and clinical significance. *Biol Chem Hoppe Seyler.* 1992; 373: 611–622.
6. **Dvorak HF.** Tumors: wounds that do not heal. Similarities between tumor stroma generation and wound healing. *N Engl J Med.* 1986; 315: 1650–9.
7. **Sha J, Zhou Z, Li J, et al.** Identification of testis development and spermatogenesis-related genes in human and mouse testes using cDNA arrays. *Mol Hum Reprod.* 2002; 8: 511–7.
8. **Tajima K, Obata Y, Tamaki H, et al.** Expression of cancer/testis (CT) antigens in lung cancer. *Lung Cancer.* 2003; 42: 23–33.
9. **Andreasen PA, Egelund R, Petersen HH.** The plasminogen activation system in tumor growth, invasion, and metastasis. *Cell Mol Life Sci.* 2000; 57: 25–40.
10. **Laufs S, Schumacher J, Allgayer H.** Urokinase-receptor (u-PAR): an essential player in multiple games of cancer: a review on its role in tumor progression, invasion, metastasis, proliferation/dormancy, clinical outcome and minimal residual disease. *Cell Cycle.* 2006; 5: 1760–71.
11. **Lakka SS, Gondi CS, Dinh DH, et al.** Specific interference of urokinase-type plasminogen activator receptor and matrix metalloproteinase-9 gene expression induced by double-stranded RNA results in decreased invasion, tumor growth, and angiogenesis in gliomas. *J Biol Chem.* 2005; 280: 21882–92.
12. **Ellerbroek SM, Stack MS.** Membrane associated matrix metalloproteinases in metastasis. *Bioessays.* 1999; 21: 940–9.
13. **Turpeenniemi-Hujanen T.** Gelatinases (MMP-2 and -9) and their natural inhibitors as prognostic indicators in solid cancers. *Biochimie.* 2005; 87: 287–97.
14. **Roshy S, Sloane BF, Moin K.** Pericellular cathepsin B and malignant progression. *Cancer Metastasis Rev.* 2003; 22: 271–86.
15. **Schmitt M, Janicke F, Moniwa N, et al.** Tumor-associated urokinase-type plasminogen activator: biological and clinical significance. *Biol Chem Hoppe Seyler.* 1992; 373: 611–22.